Electrophoresis of DNA on a disordered two-dimensional substrate

C. J. Olson Reichhardt and C. Reichhardt
Theoretical Division and Center for Nonlinear Studies, Los Alamos National Laboratory, Los Alamos, New Mexico 87545, USA
(Received 19 March 2005; revised manuscript received 20 August 2006; published 13 November 2006)

We propose a method for electrophoretic separation of DNA in which adsorbed polymers are driven over a disordered two-dimensional substrate which contains attractive sites for the polymers. Using simulations of a model for long polymer chains, we show that the mobility increases with polymer length, in contrast to gel electrophoresis techniques, and that separation can be achieved for a range of length scales. We demonstrate that the separation mechanism relies on steric interactions between polymer segments, which prevent substrate disorder sites from trapping more than one DNA segment each. Since thermal activation does not play a significant role in determining the polymer mobility, band broadening due to diffusion can be avoided in our separation method.

DOI: 10.1103/PhysRevE.74.051908 PACS number(s): 87.15.Tt, 87.14.Gg, 87.15.Aa

I. INTRODUCTION

The development of new methods for efficiently separating charged biopolymers by length has been an area of significant recent activity due to the fact that strategies for genome sequencing are based on sorting DNA fragments by size [1]. Simple charge-based sorting is not possible because the increase in electrostatic force on longer molecules with greater total charge is exactly offset by a corresponding increase in hydrodynamic drag [2]. Instead, separation is achieved using techniques such as gel electrophoresis, in which longer molecules are slowed relative to shorter ones due to interactions with cross links in the gel. Gel and capillary electrophoretic techniques are limited to DNA strands smaller than 4×10^4 base pairs (bp) in length [3]; the mobility saturates for longer strands, and sufficiently large strands fail to pass through the gel at all. There is a need for separation of strands up to 1×10^6 bp, and thus new techniques which can sort longer molecules are of particular interest [4]. The motion of elastic strings through random media is also of general interest for a wide range of systems including magnetic domain wall motion, vortex lattice motion in superconductors, and charge density waves.

Several recent proposals for electrophoretic techniques move away from the traditional media of gels and polymers and instead take advantage of advances in nanolithography to create microstructured devices for separation [5–15]. The sorting effectiveness of these techniques is limited by the relative size of the nanofabricated structure and the polymers to be sorted, making it necessary to fabricate a separate device for each size range of interest. In contrast, Seo *et al.* [16] proposed an adsorption-based separation technique that could permit the sorting of polymers which vary in size by three orders of magnitude. When the ionic strength of the buffer solution is altered [17], the DNA is partially adsorbed onto a clean surface, forming a series of loops which extend into the solution and trains which are adsorbed on the substrate. It has been proposed that separation occurs because the longer polymers have a larger number of train segments, and thus experience a greater retardation of their motion [18,19].

The quasi-two-dimensional geometry considered in Ref. [16] is very appealing for separation purposes, in part because adsorbed polymers spread out significantly into flat "pancakes" [20] compared to their coiled three-dimensional configurations, permitting better coupling to length differences. The sorting mechanism in Ref. [16] precludes complete adsorption, however, since there is no separation for fully desorbed or fully adsorbed polymers. This limits the length range that can be processed, since if the surface is strongly attractive to DNA, long DNA chains fully adsorb and separation by length is lost. If instead the surface weakly attracts DNA, short chains desorb from the surface and cannot be separated [21].

Here we propose an alternative sorting technique for long DNA strands in which the polymers are fully adsorbed on the surface. To permit separation, we spatially modify the surface, but instead of using posts or other impenetrable barriers, we consider randomly spaced pinning sites which temporarily retard the motion of the polymer, yet still allow it to pass through. Such pinning could be created via the manipulation of lipid bilayer membranes [22] or surface patterning [23]. We show that, in this geometry, longer polymers are more mobile than shorter ones, in contrast to typical separation methods where longer polymers move more slowly. This avoids the jamming or clogging associated with long polymers in other techniques. The steric interaction between polymer segments causes the longer polymers to be less well pinned by the random disorder than the short polymers, and allows separation by length to occur.

To demonstrate our separation mechanism, we use a simulation model that we have developed for long DNA fragments. Many of the existing simulation models for electrophoretic processes are best suited for shorter polymers [24]. Since we are concerned with polymers up to 300 μm in length, we do not attempt to simulate each atom in the polymer. Instead, we adopt a bead-spring model in which the polymer is represented by multiple beads [25] which are each spaced many persistence lengths apart. There is an entropic resistance to the stretching of the polymer segment between two beads, which is represented by a finitely extensible nonlinear spring (FENE) potential [26] that replaces the internal degrees of freedom of the polymer molecule [27]. An essential assumption of this model is that the polymer segment between beads is significantly longer than the polymer persistence length. This is in contrast to bead-stick models [28], where the distance between beads is ten or fewer actual chemical segments.

II. SIMULATION

We employ Brownian dynamics [29], permitting us to use time steps of order 0.1 ns, orders of magnitude greater than the sub-femtosecond time steps required in all-atom molecular dynamics. In this technique, the solvent is treated statistically rather than explicitly [30]. The dimensionless force on bead i in a chain L base pairs long represented by N beads is given by

$$\mathbf{F}_i = \sum_{\mathrm{NN}} \mathbf{F}_i^{FENE} + \sum_{j=1}^{N} \mathbf{F}_{ij}^{EV} + \sum_{k=i}^{N_p} \mathbf{F}_{ik}^{S} + \mathbf{F}^{E} + \mathbf{F}^{T}, \tag{1}$$

where $\mathbf{F}^{FENE}$ is the spring force along the chain, $\mathbf{F}^{EV}$ represents the excluded volume between beads, $\mathbf{F}^{S}$ is the force from a disordered substrate, $\mathbf{F}^{E}$ is the electrophoretic force, and $\mathbf{F}^{T}$ is a thermal noise term. Distances are measured in terms of σ_s, the root mean square length of the spring. Forces are expressed in terms of k_BT/σ_s. We can neglect hydrodynamic interactions since they are screened due to the proximity to the solid substrate [31,32]. Electro-osmotic effects can be controlled in the usual way by means of a high-concentration buffer [9,13,16,33]. We assume that the Debye length is considerably smaller than the distance between the beads in our model.

The force between bead i and neighboring beads is given by

$$F_i^{FENE} = \frac{-HQ}{1-(Q/Q_0)^2}\hat{\mathbf{Q}} \tag{2}$$

where $\mathbf{Q}=|\boldsymbol{l}-\boldsymbol{l}_0|$ is the elongation of the spring, $\boldsymbol{l}$ is the distance vector between two neighboring beads, $\boldsymbol{l}_0=\sigma_s\hat{\boldsymbol{l}}$ is the equilibrium spring length, Q_0 is the maximum allowable elongation, and the Hookean spring constant $H=3/\sigma_s^3$. This phenomenological spring potential [26] has the properties that it is equivalent to a Hookean spring for small Q, but becomes infinite at finite spring elongation. The persistence length l_p of double-stranded DNA is $l_p \approx 500$ Å [34]. The Kuhn length $b_k=2l_p$, giving $b_k=0.1$ μm, where we assume that the ionic strength of the buffer solution is sufficient to screen electrostatic repulsion between sections of the chain [35]. Each base pair is 0.34 nm long so one Kuhn length contains 300 bps [36]. Since we will be using a Gaussian chain model for the excluded volume interactions, which requires the chain segments between beads to be represented statistically and not deterministically, the number n of Kuhn lengths between beads must be sufficiently large (well above the bead-rod limit of $n=1$), so we take $Q_0=nb_k=1.6$ μm. This gives $n=16$ and $\sigma_s=\sqrt{n}b_k=0.4$ μm.

The excluded volume term accounts for the repulsive interaction between polymer segments when they approach each other [37,38], an effect which is more pronounced in two than in three dimensions [39]. The excluded volume interaction for beads i and j a unitless distance r_{bb} apart is taken after that used in Ref. [40], which is based on the energy penalty due to overlap of two Gaussian coils, and has the form

$$\mathbf{F}_{ij}^{EV} = -Ar_{bb}e^{-Br_{bb}^2}\hat{\mathbf{r}}_{bb} \tag{3}$$

where

$$A = \left(\frac{3}{4S_s^2}\right)^{5/2}\sigma_s v n^2 \pi^{-3/2}, \quad B = \frac{3\sigma_s^2}{4S_s^2}. \tag{4}$$

Here the size parameter $S_s^2=nb_k^2/6$ [40], while the excluded volume parameter v is taken to be $v=b_k^3$. This gives

$$A = \frac{243\sqrt{2n}}{4\pi^{3/2}}, \quad B = \frac{9}{2}. \tag{5}$$

The substrate roughness is represented by N_p finite-range parabolic pinning traps of radius $\sigma_p=0.4\sigma_s$, strength f_p, and density ρ_p. The pin size was chosen to be close to the Kuhn length. The force on bead i from pin k a distance r_{bp} away is given by

$$\mathbf{F}_{ik}^{S} = f_p\frac{r_{bp}}{\sigma_p}\Theta(\sigma_p - r_{bp})\hat{\mathbf{r}}_{bp} \tag{6}$$

where Θ is the Heaviside step function.

The electrophoretic force on each bead from an applied electric field E is

$$\mathbf{F}^{E} = qE\hat{\mathbf{y}}. \tag{7}$$

Here, $q=\lambda nb_k$ is the charge per bead, where the charge per unit length of DNA in solution is $\lambda=4.6\times10^{-10}\mathrm{C}/m$, or $0.3e^-/$Å [5]. $\mathbf{F}^T$ is the Langevin thermal noise term representing the Brownian forces. It is a δ correlated white noise process which obeys $\langle F^T\rangle=0$ and the fluctuation-dissipation theorem [41] $\langle F_i^T(t)F_j^T(t+\Delta\tau)\rangle=2k_BT\zeta^{-1}\delta_{ij}\delta(\Delta\tau)$. Here δ_{ij} is a Kronecker delta tensor and $\delta(\Delta\tau)$ is the Dirac delta function. Time is measured in units of $\tau=\zeta\sigma_s^2/(k_BT)$ and we take $\delta\tau=0.001$. ζ is the friction coefficient characterizing the viscous interaction between the bead and the solvent. We use the experimentally measured value of ζ for polymers diffusing in a bilayer, $\zeta=2.97\times10^{-7}$ N s/m [42]. Theoretically, for a polymer moving in three dimensions, $\zeta=6\pi\eta_s\sigma$, where σ is the effective bead radius and η_s is the solvent viscosity. We note that a theoretical expression for the friction coefficient in the case of a particle confined to a membrane suspended in a solvent has been developed by Saffman [43], where only a weak dependence of ζ on effective bead radius is obtained.

III. RESULTS

We first consider the velocity of the polymers over the rough substrate as a function of polymer length L. We sweep the electric field strength and find the average velocity $\langle V\rangle$ at each field value during 200 repetitions of the sweep. In Fig. 1 we plot the velocity-force curves for polymers of length ranging from $N=5$ to 100, where N is the number of beads used to model the polymer, in a sample with pinning density $\rho_p=0.8$ and strength $f_p=60$ at room temperature. In physical units, this length range is 8–160 μm, and it includes λ-phage DNA, which has a contour length of 21.2 μm [44]. A velocity of 10 corresponds to 0.3 μm/s, and an applied

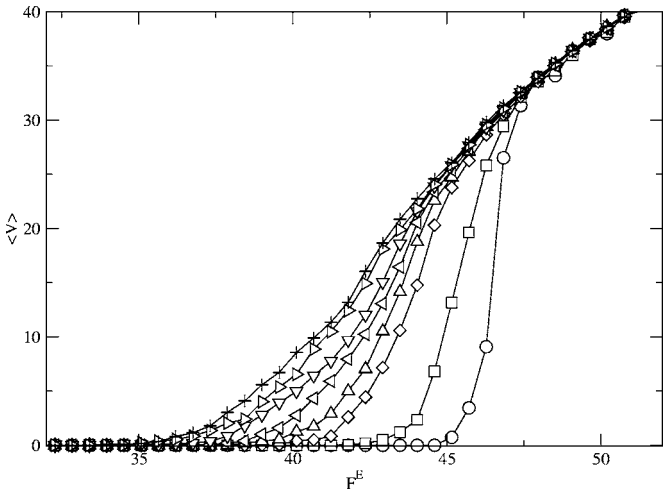

FIG. 1. Average velocity $\langle V \rangle$ versus electric field for pinning density $\rho_p=0.8$, pin strength $f_p=60$, and polymers of different lengths represented by the number of beads $N=5$ (circles), 10 (squares), 20 (diamonds), 30 (triangles up), 40 (triangles left), 50 (triangles down), 80 (triangles right), and 100 (pluses).

field of 30 corresponds to 4.16 V/cm. After the polymers depin, there is a range of driving force over which we find a nonlinear velocity-force characteristic. Within this range the shorter polymers move more slowly than the longer polymers for a given electric field strength.

Short polymers are better pinned by the underlying disorder than long polymers, and thus a higher driving force must be applied before the short polymers begin to move over the substrate. In Fig. 2 we illustrate the dependence of the critical depinning force F_c on polymer length L for a range of pinning strengths and densities. Here we define F_c as the driving force at which $\langle V \rangle = 1$. We have chosen this definition since in our technique, physical separation of the polymers will occur when the polymers are moving with different velocities. In an experiment, if the electric field were held at a value between F_c for polymers of two lengths, the two polymers will be separated since one is strongly mobile while the other is nearly immobile. As shown in Fig. 2, in each case we find that F_c drops logarithmically with increasing L, as indicated by the dashed lines. As the pinning density is reduced from $\rho=1.0$ to $\rho=0.2$, shown in Fig. 2(a), the depinning force drops and the variation of F_c with L becomes steeper, meaning that the separation resolution is enhanced. At the same time, the length range over which effective separation can be achieved drops, and thus there is a trade-off which must be considered depending on the range of sizes that are to be separated. We show the scaled length dependence of F_c/f_p in Fig. 2(b) for pinning strengths $f_p=20-80$. The pinning effectiveness drops slightly faster than the pinning strength, as indicated by the fact that the curves do not fall on top of each other. For the weakest pins, the separation effectiveness washes out above a length of $N \sim 100$.

The excluded volume interactions play the key role in the separation mechanism. What is happening physically can be understood as follows. Consider a polymer composed of only a single bead. This polymer can be completely trapped by a single pinning site. Next, consider a polymer composed of two beads. Although it is possible for the polymer to find two adjacent pinning sites such that both beads are pinned, it is more likely that one bead will be pinned while the other is still free. In this case the force from only one pin will have to hold two beads still against the electrophoretic force. If the excluded volume interactions are removed, both beads can fit inside the pin, doubling the effective pinning force. As the polymer becomes longer and is composed of more beads, the relative fraction of the polymer that is pinned decreases, provided that each pin can capture only one bead. This results in the decreased threshold for depinning and the increased mobility of the longer polymers relative to the short ones. The importance of the excluded volume interaction is that it enforces a pin occupancy of at most one bead per pin. Thus, the excluded volume interaction is what produces the decrease in F_c with polymer length. We test this by running a series of simulations without the excluded volume interaction. The depinning force F_c for this case is shown in the inset to Fig. 3, where it is clear that F_c has no significant dependence on L. The corresponding velocity-force curves are shown in Fig. 3, where it can clearly be seen that the curves lie on top of each other except for the very shortest polymers.

We stress that the separation mechanism at work here is significantly different than that which occurs in the case of impenetrable obstacles such as cross links in gels or nanofabricated posts. This can be seen by observing images of the moving polymers. A representative set of images for polymers of different length is shown in Fig. 4. The chains are moving toward the top of the figure in the $+y$ direction. Rather than forming hairpin structures, the polymers frequently form a bundle on their advancing end, and sometimes drag one or two tail segments.

For separation purposes, the polymer velocity must depend on length. This can be achieved if the depinning force of the polymers is length dependent. To demonstrate this explicitly, we run a series of simulations in which the driving

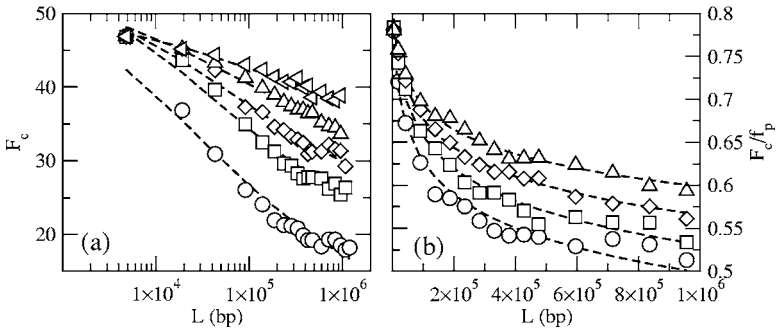

FIG. 2. (a) Critical depinning force F_c versus polymer length L on a linear-log scale for fixed $f_p=60$ and pinning density $\rho_p=0.2$ (circles), 0.4 (squares), 0.6 (diamonds), 0.8 (triangles up), and 1.0 (triangles left). Dashed lines are logarithmic fits. (b) Scaled critical depinning force F_c/f_p versus L for fixed $\rho_p=0.8$ and $f_p=20$ (circles), 40 (squares), 60 (diamonds), and 80 (triangles). Dashed lines are logarithmic fits.

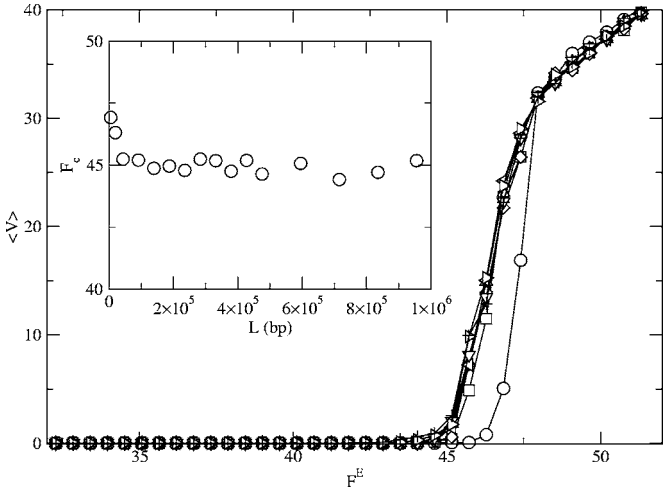

FIG. 3. Average velocity $\langle V \rangle$ versus electric field for a system with no excluded volume at pinning density $\rho_p=0.8$, pin strength $f_p=60$, and polymers of different length $N=5$ (circles), 10 (squares), 20 (diamonds), 30 (triangles up), 40 (triangles left), 50 (triangles down), 80 (triangles right), and 100 (pluses). Inset: F_c versus L for the same system.

force is held at a fixed value, and measure the average velocity $\langle V \rangle$. The results are plotted in Fig. 5 for five different values of F^E in a sample with $\rho_p=0.8$ and $f_p=60$. The velocity increases logarithmically with polymer length, as indicated by the dashed lines, and velocity variations of an order of magnitude can be achieved.

We note that in traditional gel electrophoresis techniques, diffusion is an important limiting effect, since the polymers are moving through the gel relatively slowly and depend on

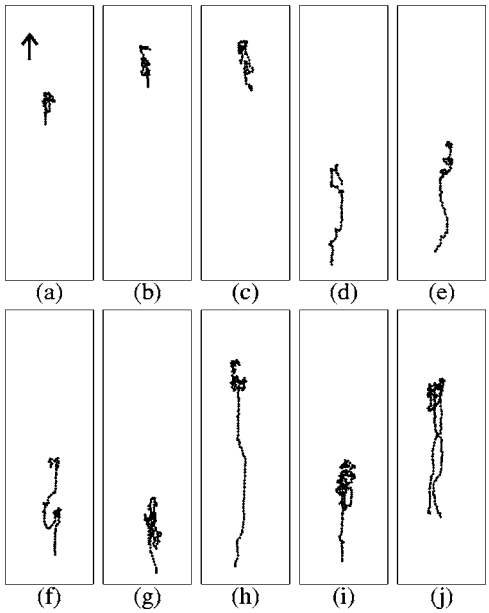

FIG. 4. Images from polymer simulation showing bead positions for length $N=$ (a) 40, (b) 50, (c) 60, (d) 70, (e) 80, (f) 90, (g) 100, (h) 125, (i) 150, (j) 175, and (k) 200. The driving force is in the $+y$ direction, toward the top of the figure, as indicated by the arrow in (a).

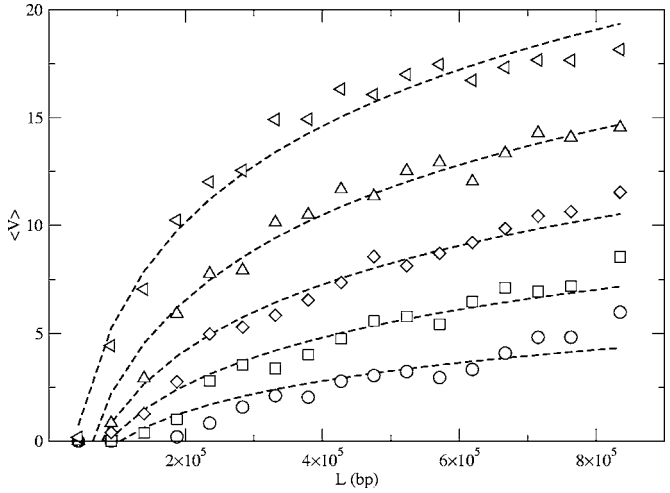

FIG. 5. (a) Velocity $\langle V \rangle$ versus polymer length L for $f_p=60$ and $\rho_p=0.8$ at different applied driving fields of $F^E=37.88$ (circles), 39.0 (squares), 40.12 (diamonds), 41.24 (triangles up), and 42.36 (triangles left). Dashed lines are logarithmic fits.

thermal fluctuations to help them translocate through the gel. This effect is particularly pronounced for long polymers, which have extreme difficulty passing through the gel at all. In contrast, in the technique proposed here, the polymers are much more mobile than they would be in a gel. The configurations and depinning of the polymers are dominated by the strong electric fields and pinning imposed, and thermal effects play essentially no role in the separation. We observe no significant thermal diffusion in our system at all. As a result, diffusive broadening of the bands can be prevented. The bands do still broaden due to the intrinsic randomness of the pinning, which causes the progress of the polymers over the substrate to be somewhat variable. To illustrate the magnitude of this broadening, in Fig. 6(a) we plot the total distance traveled by the polymers under different drives applied for a fixed period of time for 100 realizations of disorder.

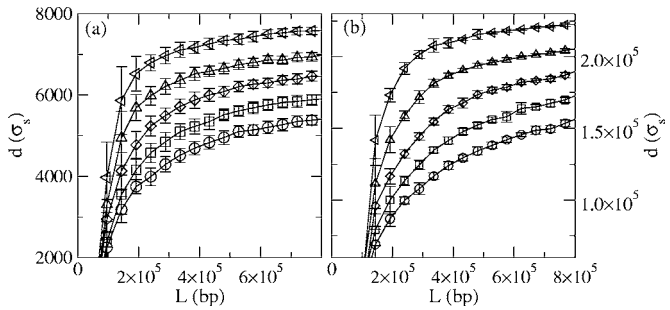

FIG. 6. (a) Distance d in units of σ_s traveled over a fixed time interval versus polymer length L for $f_p=60$ and $\rho_p=0.8$ at $F^E=37.88$ (circles), 39.0 (squares), 40.12 (diamonds), 41.24 (triangles up), and 42.36 (triangles left). Error bars indicate the spread in distance traveled over 100 realizations of disorder. (b) Distance d traveled over a longer fixed time interval versus polymer length for the same system as in (a) with $F^E=37.88$ (circles), 39.0 (squares), 40.12 (diamonds), 41.24 (triangles up), and 42.36 (triangles left). Error bars indicate the spread in distance traveled over 20 realizations of disorder.

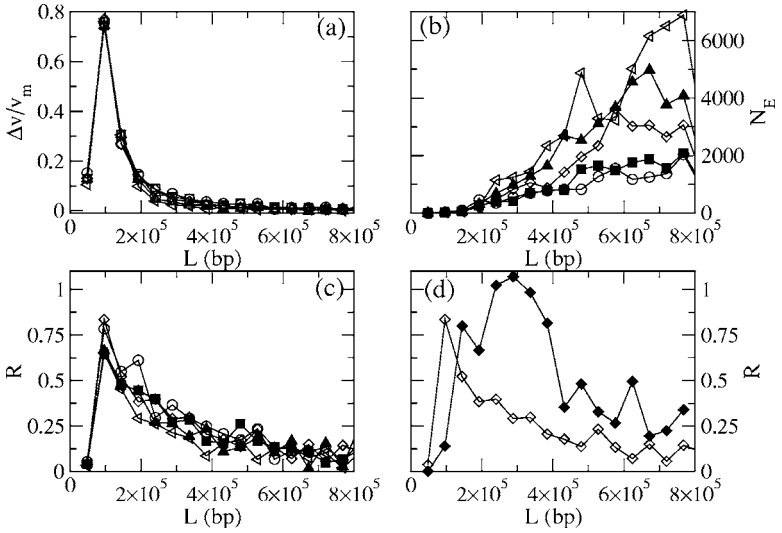

FIG. 7. (a) Selectivity $\Delta V/V_m$ from the system in Fig. 6(a) versus polymer length L for f_p=60 and ρ_p=0.8 at F^E=37.88 (circles), 39.0 (squares), 40.12 (diamonds), 41.24 (triangles up), and 42.36 (triangles left). (b) Efficiency N_E for the same system at F^E=37.88 (open circles), 39.0 (filled squares), 40.12 (diamonds), 41.24 (filled triangles up), and 42.36 (triangles left). (c) Resolution R for the same system at F^E=37.88 (open circles), 39.0 (filled squares), 40.12 (diamonds), 41.24 (filled triangles up), and 42.36 (triangles left). (d) Resolution at F^E=40.12 for (open diamonds) the system in Fig. 6(a) and (filled diamonds) the system in Fig. 6(b) where the polymers were allowed to travel a longer distance.

Error bars indicate the average maximum and minimum distances traveled by polymers of a particular length. Higher resolution can be obtained by allowing the polymers to move a larger distance through the gel, as illustrated in Fig. 6(b).

We quantify the separation power of our technique by measuring the resolution as a function of polymer length. The resolution is affected by both the selectivity and efficiency of the separation for a given length difference [45]. The selectivity $\Delta V/V_m$ is proportional to the difference in mobility for polymers of different lengths,

$$\frac{\Delta V_i}{V_m} = \frac{2(\langle V_{i+1}\rangle - \langle V_i\rangle)}{\langle V_{i+1}\rangle + \langle V_i\rangle}, \tag{8}$$

where $\langle V_i\rangle$ is the average velocity for a polymer of length L_i. Figure 7(a) shows that the selectivity for the same system in Fig. 6(a) does not vary with F^E and is highest for the shortest polymers, in the same region where Fig. 5 indicates that the $\langle V\rangle$ versus L curve has the steepest slope. The efficiency N_E is proportional to the width of the band σ_x^2 observed after the polymers have traveled a distance x,

$$N_E = \frac{x^2}{\sigma_x^2}. \tag{9}$$

As can be seen in Fig. 7(b), N_E increases with both L and F^E, consistent with the decrease in the size of the error bars at higher L and F^E shown in Fig. 6(a). The resolution R is defined as

$$R = \frac{\sqrt{\bar{N}_E}}{4}\frac{\Delta V}{V_m} \tag{10}$$

where $\bar{N}_E$ is the mean efficiency for the polymer lengths being compared. We plot R versus L in Fig. 7(c). The resolution depends more strongly on the selectivity than on the efficiency, and as a result we find that R is highest for the shortest polymers and is not a strong function of F^E. The resolution can be improved by allowing the polymers to travel a longer distance, as in Fig. 6(b). We compare the resolution for shorter and longer distances traveled in Fig. 7(d), where we find not only an enhancement of R for the longer travel distance, but also a shift in the peak value of R towards longer polymers. This suggests that the technique could be optimized for separation of the desired range of L by adjusting the distance traveled by the polymers.

IV. CONCLUSION

In summary, we have used a model developed for the simulation of long DNA segments to demonstrate a length separation mechanism for polymers adsorbed to a disordered two-dimensional substrate. Longer polymers are more mobile than short polymers, and the depinning force decreases logarithmically with polymer length. Correspondingly, the polymer velocity increases logarithmically with length. The separation mechanism arises due to the excluded volume interaction between chain segments, which serves to reduce the effectiveness of the random pinning for longer polymers. One possible experimental system in which our proposed separation mechanism could be realized is solid-supported cationic lipid membranes, where DNA is confined to two dimensions but free to diffuse in plane [31]. The pinning could be produced in the form of disorder on the supporting substrate, which would perturb the bilayer and interfere with the free diffusion of the DNA. Such disorder could potentially be produced by an experimental technique as simple as not fully cleaning the substrate before depositing the bilayer. Our proposed separation mechanism offers several advantages over existing techniques. (1) It may not be necessary to use elaborate nanofabrication methods to produce the pinning. (2) The technique can be used to separate extremely long strands of DNA which will not pass through conventional gels. (3) It may be possible to achieve high throughput since the polymers do not need to work their way around fixed impassible obstacles, but are instead only temporarily hindered by the pinning sites, and can thus achieve much higher overall mobilities than are possible in a gel, particularly for long polymers. (4) Since thermal effects do not play a significant role in the separation technique, thermal broadening of the bands by diffusion should be strongly sup-

pressed. The resolution limitation caused by band broadening from the intrinsic disorder of the substrate can be reduced by allowing the polymers to travel a longer distance during separation.

ACKNOWLEDGMENT

This work was supported by the U.S. Department of Energy under Contract No. W-7405-ENG-36.

[1] J.-L. Viovy, Rev. Mod. Phys. **72**, 813 (2000), and references therein.
[2] G. W. Slater and J. Noolandi, Biopolymers **25**, 431 (1986).
[3] J. J. Schwinefus and M. D. Morris, Macromolecules **32**, 3678 (1999).
[4] Z. Huang, J. T. Petty, B. O'Quinn, J. L. Longmire, N. C. Brown, J. H. Jett, and R. A. Keller, Nucleic Acids Res. **24**, 4202 (1996); R. Ashton, C. Padala, and R. S. Kane, Curr. Opin. Biotechnol. **14**, 497 (2003).
[5] W. Volkmuth and R. H. Austin, Nature (London) **358**, 600 (1992).
[6] T. A. J. Duke and R. H. Austin, Phys. Rev. Lett. **80**, 1552 (1998); D. Ertaş, *ibid.* **80**, 1548 (1998).
[7] S. W. Turner, A. M. Perez, A. Lopez, and H. G. Craighead, J. Vac. Sci. Technol. B **16**, 3835 (1998); J. Han, S. W. Turner, and H. G. Craighead, Phys. Rev. Lett. **83**, 1688 (1999); J. Han and H. G. Craighead, Science **288**, 1026 (2000); D. Nykypanchuk, H. H. Strey, and D. A. Hoagland, *ibid.* **297**, 987 (2002).
[8] C.-F. Chou, O. Bakajin, S. W. P. Turner, T. A. J. Duke, S. S. Chan, E. C. Cox, H. G. Craighead, and R. H. Austin, Proc. Natl. Acad. Sci. U.S.A. **96**, 13762 (1999).
[9] J. Han and H. G. Craighead, J. Vac. Sci. Technol. A **17**, 2142 (1999).
[10] J. Rousseau, G. Drouin, and G. W. Slater, Phys. Rev. Lett. **79**, 1945 (1997).
[11] O. Bakajin, T. A. J. Duke, J. Tegenfeldt, C.-F. Chou, S. S. Chan, R. H. Austin, and E. C. Cox, Anal. Chem. **73**, 6053 (2001).
[12] L. R. Huang, J. O. Tegenfeldt, J. J. Kraeft, J. C. Sturm, R. H. Austin, and E. C. Cox, Nature (London) **20**, 1048 (2002).
[13] L. R. Huang, P. Silberzan, J. O. Tegenfeldt, E. C. Cox, J. C. Sturm, R. H. Austin, and H. Craighead, Phys. Rev. Lett. **89**, 178301 (2002).
[14] M. Cabodi, Y.-F. Chen, S. W. Turner, H. G. Craighead, and R. H. Austin, Electrophoresis **23**, 3496 (2002).
[15] S. W. P. Turner, M. Cabodi, and H. G. Craighead, Phys. Rev. Lett. **88**, 128103 (2002).
[16] Y.-S. Seo, V. A. Samuilov, J. Sokolov, M. Rafailovich, B. Tinland, J. Kim, and B. Chu, Electrophoresis **23**, 2618 (2002).
[17] R. Menes, P. Pincus, R. Pittman, and N. Dan, Europhys. Lett. **44**, 393 (1998).
[18] N. Pernodet, V. Samuilov, K. Shin, J. Sokolov, M. H. Rafailovich, D. Gersappe, and B. Chu, Phys. Rev. Lett. **85**, 5651 (2000).
[19] H. Luo and D. Gersappe, Electrophoresis **23**, 2690 (2002).
[20] P.-G. de Gennes, *Scaling Concepts in Polymer Physics* (Cornell University Press, Ithaca, N.Y., 1979).
[21] Y.-S. Seo, H. Luo, V. A. Samuilov, M. H. Rafailovich, J. Sokolov, D. Gersappe, and B. Chu, Nano Lett. **4**, 659 (2004).
[22] L. A. Kung, L. Kam, J. S. Hovis, and S. G. Boxer, Langmuir **16**, 6773 (2000); R. N. Orth, J. Kameoka, W. R. Zipfel, B. Ilic, W. W. Webb, T. G. Clark, and H. G. Craighead, Biophys. J. **85**, 3066 (2003); K. Morigaki, K. Kiyosue, and T. Taguchi, Langmuir **20**, 7729 (2004); C. K. Yee, M. L. Amweg, and A. N. Parikh, J. Am. Chem. Soc. **126**, 13962 (2004).
[23] R. K. Workman and S. Manne, Langmuir **18**, 661 (2002).
[24] M. Olvera de la Cruz, J. M. Deutsch, and S. F. Edwards, Phys. Rev. A **33**, 2047 (1986); J. M. Deutsch, Phys. Rev. Lett. **59**, 1255 (1987); J. M. Deutsch, Science **240**, 922 (1988); J. M. Deutsch and T. L. Madden, J. Chem. Phys. **90**, 2476 (1989); E. O. Schaffer and M. Olvera de la Cruz, Macromolecules **22**, 1351 (1989).
[25] P. E. Rouse, J. Chem. Phys. **21**, 1272 (1953).
[26] H. R. Warner, Ind. Eng. Chem. Fundam. **11**, 379 (1972).
[27] P. S. Doyle, E. S. G. Shaqfeh, and A. P. Gast, J. Fluid Mech. **334**, 251 (1997).
[28] G. S. Grest and K. Kremer, Phys. Rev. A **33**, R3628 (1986).
[29] D. L. Ermak and J. A. McCammon, J. Chem. Phys. **69**, 1352 (1978).
[30] J. W. Rudisill and P. T. Cummings, J. Non-Newtonian Fluid Mech. **41**, 275 (1992).
[31] B. Maier and J. O. Rädler, Phys. Rev. Lett. **82**, 1911 (1999).
[32] O. B. Bakajin, T. A. J. Duke, C. F. Chou, S. S. Chan, R. H. Austin, and E. C. Cox, Phys. Rev. Lett. **80**, 2737 (1998).
[33] J. Han and H. G. Craighead, Anal. Chem. **74**, 394 (2002).
[34] H. R. Reese and B. H. Zimm, J. Chem. Phys. **92**, 2650 (1990).
[35] P. D. Patel and E. S. G. Shaqfeh, J. Chem. Phys. **118**, 2941 (2003).
[36] D. Long and J. L. Viovy, Phys. Rev. E **53**, 803 (1996).
[37] R. L. C. Akkermans and W. J. Briels, J. Chem. Phys. **114**, 1020 (2001).
[38] K. S. Kumar and J. R. Prakash, Macromolecules **36**, 7842 (2003).
[39] G. W. Slater and S. Y. Wu, Phys. Rev. Lett. **75**, 164 (1995).
[40] R. M. Jendrejack, J. J. de Pablo, and M. D. Graham, J. Chem. Phys. **116**, 7752 (2002).
[41] R. Kubo, Rep. Prog. Phys. **29**, 255 (1966).
[42] D. J. Olson, J. M. Johnson, P. D. Patel, E. S. G. Shaqfeh, S. G. Boxer, and G. G. Fuller, Langmuir **17**, 7396 (2001).
[43] P. G. Saffman and M. Delbruck, Proc. Natl. Acad. Sci. U.S.A. **72**, 3111 (1975).
[44] C.-C. Hsieh, L. Li, and R. G. Larson, J. Non-Newtonian Fluid Mech. **113**, 147 (2003).
[45] S. L. Petersen and N. E. Ballou, Anal. Chem. **64**, 1676 (1992).